Highly Efficient Separation of Ultratrace Radioactive Copper Using a Flow Electrolysis Cell

Yumi Sugo, Shin-Ichi Ohira,* Hinako Manabe, Yo-hei Maruyama, Naoaki Yamazaki, Ryoma Miyachi, Kei Toda, Noriko S. Ishioka, and Masanobu Mori*
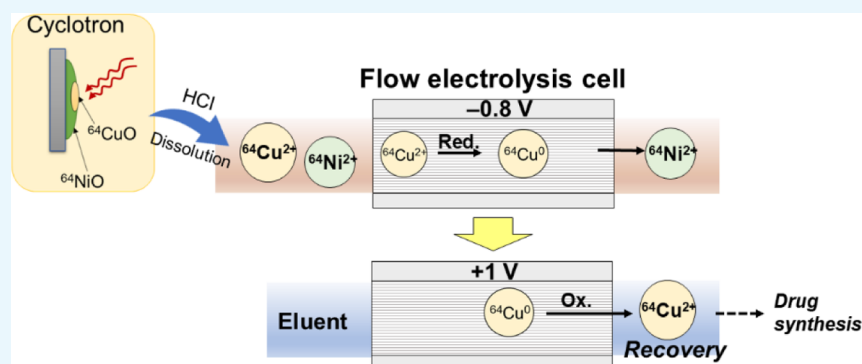
Read Online

ACCESS | Metrics & More | Article Recommendations | Supporting Information

ABSTRACT: Preparing compounds containing the radioisotope ^{64}Cu for use in positron emission tomography cancer diagnostics is an ongoing area of research. In this study, a highly efficient separation method to recover ^{64}Cu generated by irradiating the target ^{64}Ni with a proton beam was developed by employing a flow electrolysis cell (FE). This system consists of (1) applying a reduction potential for the selective adsorption of ^{64}Cu from the target solution when dissolved in HCl and (2) recovering the ^{64}Cu deposited onto the carbon working electrode by desorbing it from the FE during elution with 10 mmol/L HNO_3, which applies an oxidation potential. The ^{64}Cu was selectively eluted at approximately 30 min under a flow rate of 0.5 mL/min from the injection to recovery. The newly developed flow electrolysis system can separate the femtomolar level of ultratrace radioisotopes from the larger amount of target metals as an alternative to conventional column chromatography.

Cancer is a major cause of death in economically developed countries.[1,2] Thus, there have been many studies on cancer treatment methods such as surgery,[3] radiotherapy,[4] and chemotherapy.[5] Advanced cancer is characterized by invasion and metastasis; therefore, the early detection of cancer is important to improve outcomes. Many techniques that enable an early diagnosis of cancer have been developed.[6−10] However, when patients are exposed to X-rays and radiation for diagnosis, it sometimes places a heavy burden on the body. Positron emission tomography (PET)[11] is one of the less burdensome diagnostic imaging methods. PET can measure primary and metastatic lesions of cancer throughout the whole body at one time with relatively small exposure to the radiation, while X-ray examination measures partial parts of the human body such as lungs and stomach with a single measurement. In PET, L-methionine labeled with ^{11}C (^{11}C-MET) or glucose labeled with ^{18}F (^{18}F-FDG) is injected into the body as a radioactive isotope. These compounds can be prepared with a small cyclotron in hospitals. When ^{11}C-MET[12] and ^{18}F-FDG[13] accumulate in cancer cells, they emit radiation, allowing PET to measure the location and size of the tumor. However, because these radioactive elements have a short half-

life (^{18}F: 109.77(5) m; ^{11}C: 20.364(14) m), they are not suitable for use with drugs, such as antibodies, that take a long time to accumulate in tumors. If radiopharmaceuticals could be rapidly prepared and, moreover, entirely in a closed flow system, i.e., from the separation through drug synthesis, then the loss of radioactivity could be alleviated, thereby contributing to more effective diagnosis and treatment methods.

The use of ^{64}Cu, a copper radioisotope with a moderately long half-life (12.701(2) h), has recently been investigated as one of RI alternating to ^{18}F or ^{11}C.[14−16] Because copper can be stably complexed with a variety of compounds, including 1,4,7,10-tetraazacyclododecane-1,4,7,10-tetraacetic acid (DOTA), it has been widely used in clinical trials of PET
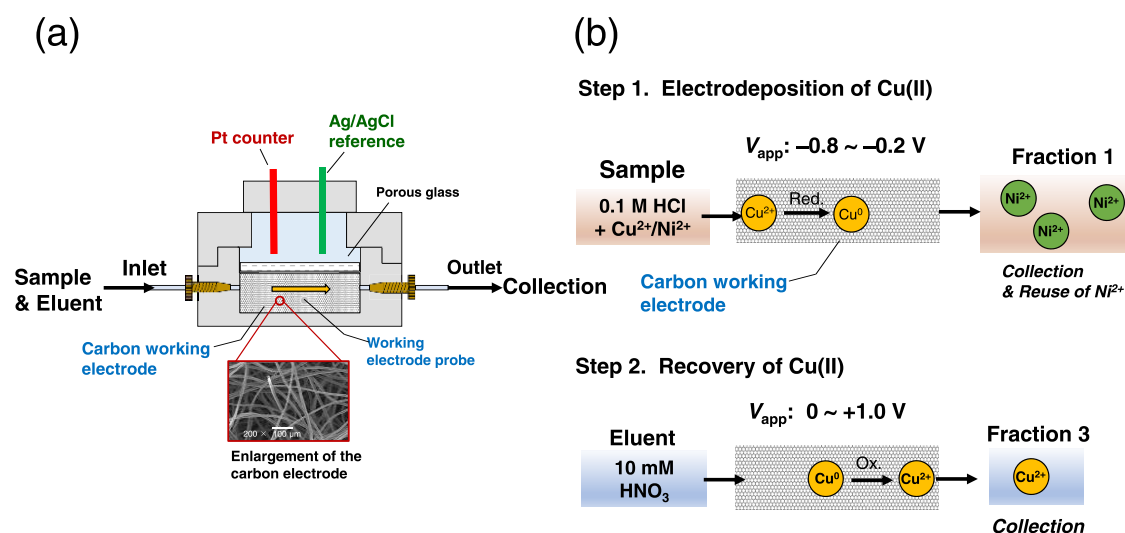
(a)

(b)
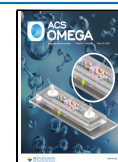
Figure 1. Schematic of the flow electrolysis cell: (a) overview of the FE and (b) electrodeposition and recovery of Cu^{2+} from the Ni^{2+} matrix.

diagnostics.[17] Also, Yoshii et al. reported that Cu-cetuximab was injected into a model mouse and successfully visualized pancreatic cancer smaller than 1 cm by a PET system equipped with a three-dimensional (3D) radiation detector.[18] Thus, utilizing ^{64}Cu has increased as the attractive RI metal in PET diagnosis.

However, because the radiation intensity of the produced nuclides has decreased by the time of clinical use, the shortest possible process time from ^{64}Cu production to drug synthesis (as described below) has been required. The production steps include:

(1) Production of pico- or nanomole levels of ^{64}Cu by irradiating [64]NiO or [64]Ni metal with a proton beam.
(2) Dissolution of the irradiated samples with hydrochloric acid and heating.
(3) Separation of ^{64}Cu from the [64]Ni matrix by column chromatography.
(4) Removal of hydrochloric acid by evaporation to dryness.

The process (1) takes 1−5 h, depending on the amount of RI−Cu required.[19,20] The processes (2)−(4) related to the separation and purification of ^{64}Cu take approximately 2.5−4 h, i.e., 1−2 h in process (2), 15−30 min in process (3), and 1−2 h in process (4), though the required times for the processes are different among the research groups.[19,20] The attenuation factor of the [64]Cu (f) during processes (2)−(4) estimated from eq 1 is reduced to 0.80−0.87, assuming an initial radioactivity of 1

$$f = A/A_0 = (1/2)^{t/T} \tag{1}$$

where T is half-life, t is the attenuation time, A_0 is the initial radioactivity, and A is the radioactivity to attenuation time.

The manufacturing process can be fully automated to avoid radioactive contamination and radiation exposure to workers.[21] However, to prevent the loss of radiation intensity, rapid and highly efficient separation, purification, and drug synthesis methods are required.

Our group recently developed a drug synthesis process using an electrodialytic ion-transfer device (ITD).[22] This device was first developed by Ohira et al.[23] and has been applied to extract inorganic anions,[24] enable chromium speciation,[25] and separate weak acids.[26] The ITD was used to demonstrate in-line probe synthesis using DOTA and 1.0 pmol/L [64]Cu^{2+}. The

advantage of this process is that the desired drug can more rapidly be obtained because it eliminates the evaporation to dryness step, which takes time to completely remove the strong acid in the aqueous solution. However, in the previous work, the separation of ^{64}Cu from a large amount of [64]Ni matrix in the irradiated solid sample was still required.

In the current study, we developed an effective technique for separating ^{64}Cu from the [64]Ni matrix using electrolysis instead of the conventional method in which ^{64}Cu is separated from [64]Ni via a chelating or an ion-exchange resin column; however, the ^{64}Cu product still needs to be concentrated after separation. Electrolysis can selectively separate ^{64}Cu from the [64]Ni matrix by controlling the redox potential in a handheld-sized flow electrolysis cell (FE). The separation is based on the electrochemical nature of Cu, which preferentially undergoes reduction compared with Ni.[27] The FE adsorbs zerovalent Cu (Cu^0) and eliminates the Ni matrix by applying a reduction potential; divalent Cu (Cu^{2+}) is then desorbed by applying an oxidation potential during which acid eluent is flowed through the FE. This study preliminarily reports that the flow electrolysis method can achieve a highly efficient separation of ultratrace ^{64}Cu produced from irradiating [64]NiO with a proton beam under conditions that were optimized for the stable isotope Cu^{2+}.

■ EXPERIMENTAL SECTION

Flow Electrolysis Cell. In this initial investigation of separating Cu from Ni via electrolysis, we employed the VF2 flow electrolysis cell from EC Frontier, Co., Ltd. (Kyoto, Japan) (Figure 1a). The working electrode was a carbon felt electrode (Φ18 mm, volume: 130 mm³, effective surface area: 1900 cm²) because it enabled the efficient adsorption of the target element. The electrode was fabricated from high-density carbon fibers; the fibers are intertwined with each other, as shown in the scanning electron microscopy (SEM) image in Figure S1. Copper that is passed through the FE when a reduction potential is applied adsorbs to the surface of the fiber electrode (Figures 1 and S1). The current variations when applying the constant voltage to the FE for each faction were monitored by connecting the digital multimeter (PC7000, Sanwa Electric Instrument, Co., Ltd. Tokyo, Japan) to the electrodes of the FE. The variations were displayed by a PC
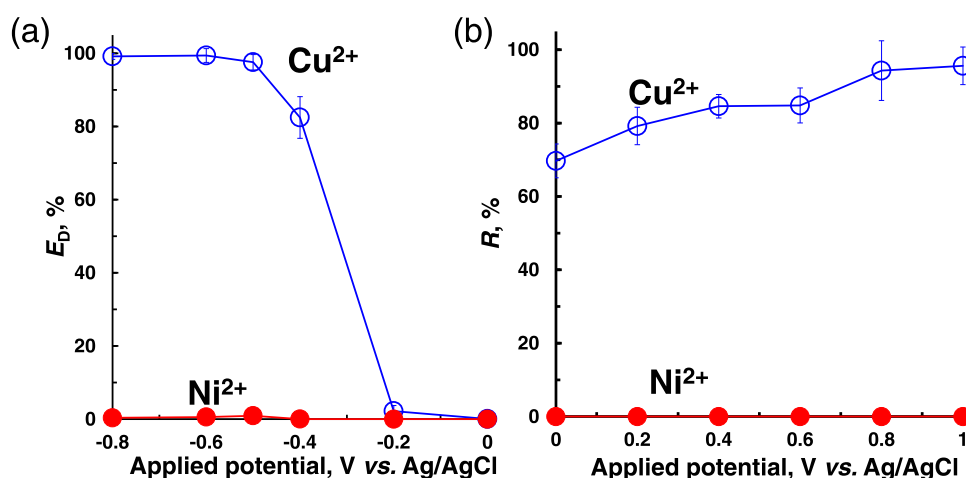
Figure 2. Effects of applied potential on (a) electrodeposition rate (E_D) of Ni^{2+} and Cu^{2+} by applying a negative potential and (b) recovery (R). Injected solution: (a) 200 μg/L $Cu(NO_3)_2$ and 200 mg/L $Ni(NO_3)_2$ in 0.1 mol/L HCl, (b) 10 mmol/L HNO_3. Flow rate: 0.5 mL/min in both the electrodeposition and recovery operations. Sample volume: 5 mL. A volume of 10 mmol/L HNO_3 was used to flush out the residue (F2): 5 mL. A volume of 10 mmol/L HNO_3 was used to desorb the Cu from the FE (F3): 5 mL.

that installed the PC Link 7 version 4.1 (Sanwa Electric Instrument, Co., Ltd.).

Procedures. Applying a reduction potential to the FE reduced the Cu^{2+} and deposited it onto the working electrode as a simple substance. Because of the difference in standard potentials ($E°_{Cu^{2+}/Cu}$ = +0.340 V, $E°_{Ni^{2+}/Ni}$ = −0.257 V),[28] the Ni matrix was kept as its ionic form, Ni^{2+}. Applying an oxidation potential with flowing 10 mmol/L HNO_3 eluted the deposited Cu. A schematic of the procedure is provided in Figure 1b.

In this study, we defined a four-step procedure as follows: the adsorption of Cu^{2+} to the FE (fraction 1, F1); flushing remaining sample solution from the FE (fraction 2, F2); recovery of Cu^{2+} from the FE (fraction 3, F3); and washing the residue from the FE (fraction 4, F4). The effluent of each fraction was separately collected and analyzed to evaluate the performance.

The electrodeposition rates (E_D) of Cu^{2+} and Ni^{2+} were estimated by eq 2

$$E_D \ (\%) = (n_{int} - n_{F1})/n_{int} \times 100 \tag{2}$$

where n_{int} (mol) is the initial amount of metal (Cu^{2+} or Ni^{2+}), and n_{F1} (mol) is the amount in the effluent that passed through the FE (i.e., F1).

The amount of Cu^{2+} adsorbed by the FE (n_{ads}, mol) was estimated by eq 3

$$n_{ads} = n_{int} - n_{F1} \tag{3}$$

The recovery (R) of Cu^{2+} that was adsorbed by the FE was calculated using eq 4

$$R \ (\%) = n_{F3}/n_{ads} \times 100 \tag{4}$$

where n_{F3} (mol) is the amount of metal in the effluent when eluting with 10 mmol/L HNO_3 (F3).

Optimization of Cu Separation Conditions in a Cold Test. The experimental conditions applied voltage and flow rate were optimized with a stable isotope experiment cold test. The sample solutions containing stable isotopes were prepared from a copper standard solution ($Cu(NO_3)_2$ in 0.1 mol/L HNO_3) and a nickel standard solution ($Ni(NO_3)_2$ in 0.1 mol/L HNO_3) (Fujifilm Wako Pure Chemical Industries, Tokyo, Osaka). The stable isotope samples were 0.1 mol/L HCl

solutions containing 200 μg/L Cu^{2+} and 200 mg/L Ni^{2+}. The samples were flowed into the FE using a peristaltic pump at a rate of 0.5−1.0 mL/min. For Cu^{2+} adsorption, −0.8−0 V (vs Ag/AgCl) was applied to the FE; for its recovery, 0−1.0 V (vs Ag/AgCl) was applied. The voltage applied to the FE was controlled by a potentiostat (HA-151B, Hokuto Denko, Co., Ltd. Tokyo, Japan). The concentrations of Cu^{2+} and Ni^{2+} in the solution eluted from the FE were determined by a flame atomic absorption spectrometry (AAnalyst 200, Perkin Elmer, Waltham, MA) and inductively coupled plasma mass spectrometry (ICP-MS, Agilent 7500cx ICP-MS, Agilent Technology, Santa Clara, CA). Their analytical conditions are summarized in Table S1.

Sample Preparation in a Hot Test. ^{64}Cu was obtained by irradiating the isotopically enriched ^{64}NiO target (Isoflex, San Francisco, CA) with a proton beam at Takasaki Ion Accelerators for Advanced Radiation Application facility in the National Institute for Quantum Science and Technology, Takasaki, Japan. The irradiated sample was dissolved in HCl with heating, and the generated ^{64}Cu was separated as described previously.[29,30] In the current study, as a tracer of the Ni matrix, ^{57}Ni (half-life: 35.60(6) h) was prepared as follows: (1) proton beam irradiation of natural Ni metal, (2) dissolution of the irradiated Ni in 6 mol/L HCl with heating, (3) evaporation to dryness, and (4) dissolution in ultrapure water. The initial concentrations of the test solution were 300 fmol/L ^{64}Cu and 3.1 mmol/L Ni (including 400 fmol/L ^{57}Ni as the tracer) in 0.1 mol/L HCl.

Separation of ^{64}Cu in a Hot Test. Prior to the electrodeposition of ^{64}Cu, 0.1 mol/L HCl was flowed into the FE, applying −0.8 V (vs Ag/AgCl) to the FE by a potentiostat. Next, the test solution of 5 mL was flowed into the FE using a peristaltic pump at a flow rate of 0.5 mL/min. Subsequently, 5 mL of 0.01 mol/L HNO_3 was flowed into the FE under the same conditions; this procedure gave F1. The sample solution remaining in the FE was then flushed out with 10 mmol/L HNO_3 (5 mL) at a flow rate of 0.5 mL/min while applying −0.8 V. This procedure produced F2. The Cu deposited in the FE was eluted with 0.01 mol/L HNO_3 (5 mL) at a flow rate of 0.5 mL/min while applying +1.0 V (vs Ag/AgCl). This procedure gave F3. Finally, 0.1 mol/L HCl (5
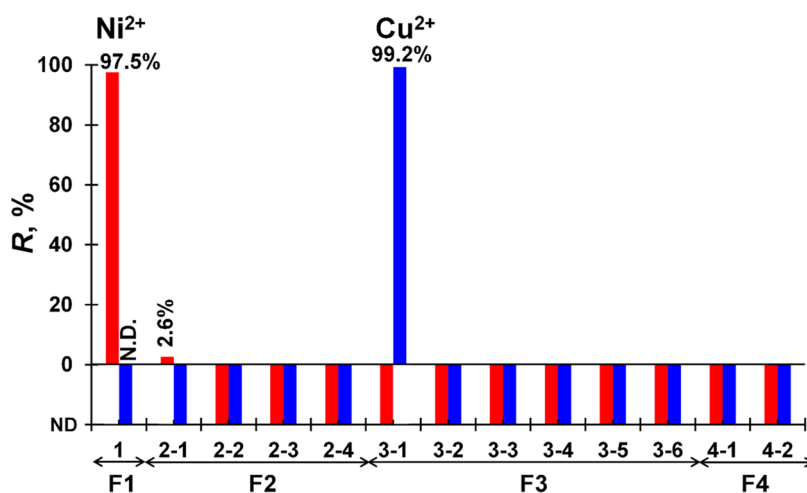
Figure 3. Recoveries (R) of Ni^{2+} and Cu^{2+} eluted in the four fractionation procedures. A sample volume of 5 mL (0.1 mol/L HCl containing 20 μg/L Cu^{2+} and 200 mg/L Ni^{2+}) was flowed into the FE (F1); 20 mL of 10 mmol/L HNO_3 was used to flush the sample residue from the FE (F2); 20 mL of 10 mmol/L HNO_3 was used to elute the Cu from the FE (F3), and 10 mL of 0.1 mol/L HCl was used to wash the FE (F4). Flow rate: 0.5 mL/min. Applied voltage: (F1 and F2) -0.8 V, (F3) $+1.0$ V, and (F4) 0 V.

mL) was used to flush any residue from the FE in preparation for the next test. This procedure generated F4.

The radioactivity of ^{64}Cu and ^{57}Ni in each fraction was measured by a NaI (Tl) scintillation detector (AccuFLEX γ 7001, Hitachi Co., Ltd.). The chemical compositions of the effluent samples that were collected after electrodeposition (F1) and after recovery (F3) were measured by a Ge semiconductor detector coupled to a multichannel analyzer (7800 MCA, Seiko EG&G).

RESULTS AND DISCUSSION

Selective Deposition and Recovery of Stable Cu in the Cold Test. In the present method, the applied potential is the key to enable the separation. Thus, the applied potential was first optimized by the cold test. The electrodeposition of 200 μg/L Cu^{2+} and 200 mg/L Ni^{2+} onto the working electrode in the FE was observed when applying a reduction potential in the range of $-0.8–0$ V. As shown in Figure 2a, more than 97% of the Cu^{2+} was adsorbed to the FE over the range of -0.8 to -0.5 V, while almost all of the Ni^{2+} was excluded from adsorption. As mentioned above, this result was expected because zerovalent Cu is adsorbed onto the working electrode when applying a reduction potential, while divalent Ni flows through the FE.

The deposition and recovery of Cu in the FE did not significantly change over the flow rate range of 0.2–1.0 mL/min (Figure S2). Actually, even at a flow rate of 2.0 mL/min, the effective electrodeposition of Cu^{2+} was achieved (Figure S3). However, the slight deposition of Ni^{2+} to FE or the unstable recovery of Cu^{2+} was obtained. In the hot test, the flow rate was set to 0.5 mL/min to ensure quantitative and stable Cu^{2+} adsorption onto the working electrode.

We next attempted to desorb the Cu^{2+} that was deposited onto the working electrode. The eluent was 10 mmol/L HNO_3 and was flowed at 0.5 mL/min. Cu was eluted even without the applied potential because the Cu deposited in the FE was dissolved by the HNO_3. The best recovery efficiency of Cu^{2+} was obtained when $+1.0$ V was applied to the FE (Figure 2b), where the R estimated from eq 3 was 95 ± 5%.

The concentration of HNO_3 as the eluent was tested at 1 and 100 mmol/L, and the Cu was completely eluted in the

range from 10 to 100 mmol/L solution. However, the HNO_3 concentration should be as low as possible considering the electrical load on the FE and the drug synthesis after recovery. From these results, the optimal applied voltage (V_{app}) was concluded to be -0.8 V for the deposition of Cu in the FE, a V_{app} of $+1.0$ V for recovery, 10 mmol/L HNO_3 as the eluent, and a sample and eluent flow rate of 0.5 mL/min. In addition, the eluent to recover Cu^{2+} deposited into the FE can be used by a lower acid concentration compared to the column chromatographic method (e.g., >0.1 M HCl).[19,20,31] In this method, the Cu recovery from the FE can also be obtained by HCl, citric acid, or acetic acid (10 mM each), as shown in Figure S4.

Next, we optimized the volumes flowed during flushing (F2), Cu recovery (F3), and washing (F4) when 5 mL of sample containing Cu^{2+} and Ni^{2+} was flowed through the FE (F1). The solution volume directly affects the concentration of ^{64}Cu in the separated solution. It is also important to minimize the radioactive waste. Each fraction was separately collected every 5 mL. As shown in Figure 3, no Cu^{2+} was eluted in F1 or F2 while Ni^{2+} flowed through the system and was present in F1 and F2. The Cu^{2+} deposited in the FE was almost entirely eluted in the first 5 mL of HNO_3 (F3). The Ni^{2+} and Cu^{2+} in the effluents collected in the other fractions were below the quantification limits in the ICP-MS used in this study. The volume flowed for each fraction was 5 mL each from F2 to F4. The average concentrations of metals for each fraction were 195.1 ± 4.1 mg/L of Ni^{2+} in F1, 5.2 ± 0.8 mg/L of Ni^{2+} in F2, and 198.4 ± 1.1 μg/L of Cu^{2+} in F3 at three consecutive operations (Table S2).

In the present method, the time from the injection (F1) to recovery (F3) of ^{64}Cu was 30 min at a flow rate of 0.5 mL/min, which is almost unchanged compared to that of the conventional method with column chromatography. By contrast, the elution of ^{64}Cu from the FE could easily be achieved by eluent with a lower concentration of strong acid or a weaker acid (Figure S4), compared to the eluent used in the column chromatographic method.[19,20,31] The electrochemical oxidation/reduction may facilitate copper adsorption and desorption of Cu to the FE. The property may contribute to omitting evaporation to dryness for conversion to weak acids

for radiolabeling in the conventional method, which requires the most time for separation and recovery. If the evaporation to dryness is skipped, the attenuation of ^{64}Cu (f) estimated by eq 1 from the time of the dissolution of the irradiated sample and separation to recovery by the present method can be suppressed to 0.87−0.88.

We further monitored the variation in current as the applied potential during the entire operation. As shown in Figure S5, the current was greatly reduced when flowing 0.1 mol/L HCl containing Cu^{2+} and Ni^{2+} (F1). The reduction was larger than when flowing the blank solution (0.1 mol/L HCl only). The reduction of Cu^{2+} is related to the presence of protons in an acidic solution. When flushing the residue from the FE by flowing 10 mmol/L HNO_3 (F3), the current was increased to −200 μA, which was similar to that of the blank. A rapid increase in current was observed when switching the polarity from negative to positive potentials to desorb the Cu from the FE (F3), but the current exponentially decreased and finally plateaued at approximately 0.5 μA.

Hot Test for Electrodeposition and Recovery of the Radioisotope ^{64}Cu. A hot test with the radioisotope was performed. Radioisotopes can be detected even at the femtomolar level. In the present study, we found that the separation mechanism was effective at ultratrace levels of Cu. The 0.1 mol/L HCl solutions (5 mL) containing 300 fmol/L $^{64}Cu^{2+}$ (1.5 fmol) and 3.1 mmol/L Ni^{2+} (including 400 fmol/L $^{57}Ni^{2+}$ as the tracer) were injected into the FE under the optimized conditions found in the stable isotope experiments.

During $^{64}Cu^{2+}$ electrodeposition (F1), Ni^{2+} was quantitatively eluted, while $^{64}Cu^{2+}$ was selectively adsorbed in the FE
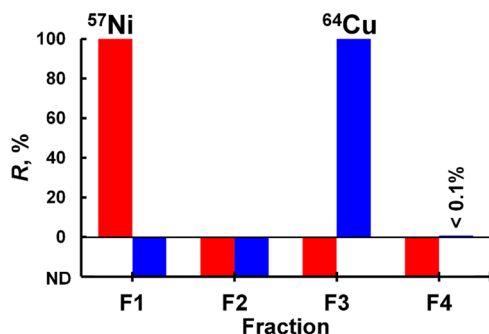

Figure 4. Recoveries of Ni matrix (^{57}Ni as the tracer) and ^{64}Cu in four fractions collected from the FE. Injected sample solutions: 300 fmol/L $^{64}Cu^{2+}$ and 3.1 mmol/L $^{64}Ni^{2+}$ (including 400 fmol/L $^{57}Ni^{2+}$ as the tracer) in 0.1 mol/L HCl. Eluent: 10 mmol/L HNO_3. Flow rate: 0.5 mL/min in both the electrodeposition and recovery operations. Sample volume: 5 mL. Volumes for F2−F4: 5 mL each.

(Figure 4). When the residue was flushed from the FE (F2), no $^{64}Cu^{2+}$ or Ni^{2+} elution was observed. This indicated that the quantitative deposition of ^{64}Cu and the elimination of ^{64}Ni quantitatively occurred during the F1 procedure. During recovery (F3), ^{64}Cu was quantitatively desorbed from the FE by changing the voltage to +1.0 V (1st ^{64}Cu recovery: 99.3%, 2nd: 100.3%). Finally, during the washing procedure without any applied voltage (F4), no $^{64}Cu^{2+}$ or Ni^{2+} elution was observed.

The obtained solutions in each protocol were also measured using a Ge semiconductor. The γ-ray spectra were obtained from the sample solution before injection into the FE (Figure

5a). The solution eluted as F1 contained ^{57}Ni (Figure 5b), while not containing ^{64}Cu. The effluent when 10 mmol/L
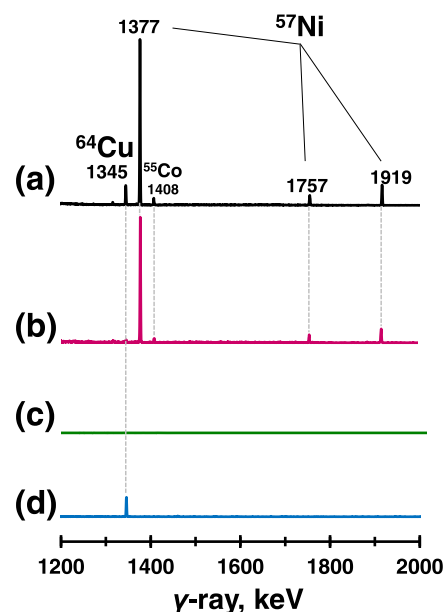

Figure 5. γ-ray spectra of FE effluents as determined by a Ge semiconductor detector. (a) A mixture of ^{57}Ni and ^{64}Cu in 0.1 mol/L HCl before injecting into the FE, (b) effluent after passing the solution through the FE by applying −0.8 V (F1), (c) effluent after flushing any remaining sample by flowing 10 mmol/L HNO_3 through the FE with applying −0.8 V (F2), and (d) effluent when flowing 10 mmol/L HNO_3 with applying +1.0 V (F3).

HNO_3 was used to flush the FE (F2) did not contain either ^{64}Cu or ^{57}Ni (Figure 5c). The F3 effluent contained only ^{64}Cu (Figure 5d). These results show that the selective and highly efficient separation of ultratrace ^{64}Cu was successfully achieved. On the other hand, ^{55}Co, which is a byproduct generated by producing ^{57}Ni, was eluted in the F1 but was not eluted in F2 or F3. Because $E°$ of Co^{2+} is −0.277 V,[28] $^{55}Co^{2+}$ was eluted by the procedures in the F1 as well as Ni^{2+}. In addition, stable Ni in the F3 was below the limit of quantification (<0.27 μg L^{-1}) by the ICP-MS used in this study.

Accordingly, in the results of the hot test, ^{64}Cu was not eluted in F2, and the separation is more efficient compared with those of the cold test. The high purity of ^{64}Cu was concluded to be recovered in F3 of the present procedures and without the need for heating and evaporation to dryness.

■ CONCLUSIONS

The flow electrolysis cell was able to selectively separate and recover femtomolar levels of ^{64}Cu. This method can thus be used as an alternative electrochemical separation method to conventional chromatographic separation. The developed method will contribute to the efficient manufacturing of PET diagnostic materials because the electrochemical procedures do not require evaporation to dryness. Therefore, we believe that this electrochemical technique will be applied in radioactive isotope medical technologies.

■ ASSOCIATED CONTENT

ⓈⒾ Supporting Information

The Supporting Information is available free of charge at https://pubs.acs.org/doi/10.1021/acsomega.2c00828.

Additional experimental details and materials, including photographs of the experimental setup; the SI is organized into the conditions and performances of AAS and ICP-MS, the overall and exploded photos of the FE and SEM imaging of the working electrode, changes in Ni^{2+} and Cu^{2+} electrodeposition rate to a negative potential, the metal concentrations eluted in F1 and F3 to the flow rate, the reproducibility at consecutive operations, the recovery of stable Cu^{2+} by several eluents, and change in current over time in the FE during Cu adsorption and desorption (PDF)

■ AUTHOR INFORMATION

Corresponding Authors

Shin-Ichi Ohira − *Department of Chemistry, Kumamoto University, Kumamoto 860-8555, Japan;* ⓞ orcid.org/0000-0002-5958-339X; Email: ohira@kumamoto-u.ac.jp

Masanobu Mori − *Faculty of Science and Technology, Kochi University, Kochi 780-8520, Japan;* ⓞ orcid.org/0000-0002-5409-6314; Email: mori@kochi-u.ac.jp

Authors

Yumi Sugo − *Department of Radiation-Applied Biology Research, Takasaki Advanced Radiation Research Institute, National Institutes for Quantum Science and Technology, Takasaki, Gunma 370-1292, Japan*

Hinako Manabe − *Faculty of Science and Technology, Kochi University, Kochi 780-8520, Japan*

Yo-hei Maruyama − *Faculty of Science and Technology, Kochi University, Kochi 780-8520, Japan*

Naoaki Yamazaki − *Graduate School of Engineering, Gunma University, Kiryu, Gunma 376-8515, Japan*

Ryoma Miyachi − *Department of Chemistry, Kumamoto University, Kumamoto 860-8555, Japan*

Kei Toda − *Department of Chemistry, Kumamoto University, Kumamoto 860-8555, Japan;* ⓞ orcid.org/0000-0001-6577-1752

Noriko S. Ishioka − *Department of Radiation-Applied Biology Research, Takasaki Advanced Radiation Research Institute, National Institutes for Quantum Science and Technology, Takasaki, Gunma 370-1292, Japan*

Complete contact information is available at:
https://pubs.acs.org/10.1021/acsomega.2c00828

Notes

The authors declare no competing financial interest.

■ ACKNOWLEDGMENTS

■ REFERENCES

(1) Jiang, Y.; Chen, S.; Hu, B.; Zhou, Y.; Liang, Z.; Jia, X.; Huang, M.; Wei, J.; Shi, Z. A comprehensive framework for assessing the impact of potential agricultural pollution on grain security and human health in economically developed areas. *Environ. Pollut.* **2020**, *263*, No. 114653.

(2) Torre, L. A.; Bray, F.; Siegel, R. L.; Ferlay, J.; Lortet-Tieulent, J.; Jemal, A. Global cancer statistics, 2012. *Ca-Cancer J. Clin.* **2015**, *65*, 87−108.

(3) Rathod, S.; Livergant, J.; Klein, J.; Witterick, I.; Ringash, J. A systematic review of quality of life in head and neck cancer treated with surgery with or without adjuvant treatment. *Oral Oncol.* **2015**, *51*, 888−900.

(4) Delaney, G.; Jacob, S.; Featherstone, C.; Barton, M. The role of radiotherapy in cancer treatment. *Cancer* **2005**, *104*, 1129−1137.

(5) Jiang, L.; Lee, S. C.; Ng, T. C. Pharmacometabonomics analysis reveals serum formate and acetate potentially associated with varying response to gemcitabine-carboplatin chemotherapy in metastatic breast cancer patients. *J. Proteome Res.* **2018**, *17*, 1248−1257.

(6) Van Schoors, M.; Caes, L.; Knoble, N. B.; Goubert, L.; Verhofstadt, L. L.; Alderfer, M. A. Systematic Review: Associations between family functioning and child adjustment after pediatric cancer diagnosis: A meta-analysis. *J. Pediatr. Psychol.* **2017**, *42*, 6−18.

(7) Liberman, M.; Sampalis, F.; Mulder, D. S.; Sampalis, J. S. Breast cancer diagnosis by scintimammography: A meta-analysis and review of the literature. *Breast Cancer Res. Treat.* **2003**, *80*, 115−126.

(8) Týčová, A.; Ledvina, V.; Klepárník, K. Recent advances in CE-MS coupling: Instrumentation, methodology, and applications. *Electrophoresis* **2017**, *38*, 115−134.

(9) Zhang, J.; Bowers, J.; Liu, L.; Wei, S.; Nagana Gowda, G. A.; Hammoud, Z.; Raftery, D. Esophageal cancer metabolite biomarkers detected by LC-MS and NMR methods. *PLoS One* **2012**, *7*, No. e30181.

(10) Barba, D.; León-Sosa, A.; Lugo, P.; Suquillo, D.; Torres, F.; Surre, F.; Trojman, L.; Caicedo, A. Breast cancer, screening and diagnostic tools: All you need to know. *Crit. Rev. Oncol. Hematol.* **2021**, *157*, No. 103174.

(11) Karas, K. H.; Baharikhoob, P.; Kolla, N. J. Borderline personality disorder and its symptom clusters: A review of positron emission tomography and single photon emission computed tomography studies. *Psychiatry Res., Neuroimaging* **2021**, *316*, No. 111375.

(12) Stewart, M. N.; Parker, M. F. L.; Jivan, S.; Luu, J. M.; Huynh, T. L.; Schulte, B.; Seo, Y.; Blecha, J. E.; Villanueva-Meyer, J. E.; Flavell, R. R.; VanBrocklin, H. F.; Ohliger, M. A.; Rosenberg, O.; Wilson, D. M. High enantiomeric excess in-loop synthesis of d-[methyl-^{11}C] methionine for use as a diagnostic positron emission tomography radiotracer in bacterial infection. *ACS Infect. Dis.* **2020**, *6*, 43−49.

(13) Hovhannisyan, N.; Dhilly, M.; Guillouet, S.; Leporrier, M.; Barré, L. Comparative analysis between [^{18}F] fludarabine-PET and [^{18}F] FDG-PET in a murine model of inflammation. *Mol. Pharmaceutics* **2016**, *13*, 2136−2139.

(14) Knighton, R. C.; Troadec, T.; Mazan, V.; Saëc, P. L.; Marionneau-Lambot, S.; Bihan, T. L.; Saffon-Merceron, N.; Bris, N. L.; Chérel, M.; Faivre-Chauvet, A.; Elhabiri, M.; Charbonnière, L. J.; Tripier, R. Cyclam-based chelators bearing phosphonated pyridine pendants for ^{64}Cu-PET imaging: Synthesis, physicochemical studies, radiolabeling, and bioimaging. *Inorg. Chem.* **2021**, *60*, 2634−2648.

(15) Sharma, A. K.; Schultz, J. W.; Prior, J. T.; Rath, N. P.; Mirica, L. M. Coordination chemistry of bifunctional chemical agents designed for applications in ^{64}Cu PET imaging for alzheimer's disease. *Inorg. Chem.* **2017**, *56*, 13801−13814.

(16) Zhou, H.; Zhang, Q.; Cheng, Y.; Xiang, L.; Shen, G.; Wu, X.; Cai, H.; Li, D.; Zhu, H.; Zhang, R.; Li, L.; Cheng, Z. ^{64}Cu-labeled melanin nanoparticles for PET/CT and radionuclide therapy of tumor. *Nanomedicine* **2020**, *29*, No. 102248.

(17) Tamura, K.; Kurihara, H.; Yonemori, K.; Tsuda, H.; Suzuki, J.; Kono, Y.; Honda, N.; Kodaira, M.; Yamamoto, H.; Yunokawa, M.; Shimizu, C.; Hasegawa, K.; Kanayama, Y.; Nozaki, S.; Kinoshita, T.;

Wada, Y.; Tazawa, S.; Takahashi, K.; Watanabe, Y.; Fujiwara, Y. ^{64}Cu-DOTA-trastuzumab PET imaging in patients with HER2-positive breast cancer. *J. Nucl. Med.* **2013**, *54*, 1869−1875.

(18) Yoshii, Y.; Tashima, H.; Iwao, Y.; Yoshida, E.; Wakizaka, H.; Akamatsu, G.; Yamaya, T.; Matsumoto, H.; Yoshimoto, M.; Igarashi, C.; Hihara, F.; Tachibana, T.; Zhang, M.; Nagatsu, K.; Sugyo, A.; Tsuji, A. B.; Higashi, T. Immuno-OpenPET: a novel approach for early diagnosis and image-guided surgery for small resectable pancreatic cancer. *Sci. Rep.* **2020**, *10*, No. 4143.

(19) van der Meulen, N. P.; Hasler, R.; Blanc, A.; Farkas, R.; Benešová, M.; Talip, Z.; Müller, C.; Schibli, R. Implementation of a new separation method to produce qualitatively improved [64]Cu. *J. Labelled Compd. Radiopharm.* **2019**, *62*, 460−470.

(20) Xie, Q.; Zhu, H.; Wang, F.; Meng, X.; Ren, Q.; Xia, C.; Yang, Z. Establishing reliable Cu-64 production process: from target plating to molecular specific tumor micro-PET imaging. *Molecules* **2017**, *22*, No. 641.

(21) Obata, A.; Kasamatsu, S.; McCarthy, D. W.; Welch, M. J.; Saji, H.; Yonekura, Y.; Fujibayashi, Y. Production of therapeutic quantities of (64)Cu using a 12 MeV cyclotron. *Nucl. Med. Biol.* **2003**, *30*, 535−539.

(22) Sugo, Y.; Miyachi, R.; Maruyama, Y.-H.; Ohira, S.-I.; Mori, M.; Ishioka, N. S.; Toda, K. Electrodialytic handling of radioactive metal ions for preparation of tracer reagents. *Anal. Chem.* **2020**, *92*, 14953−14958.

(23) Ohira, S.-I.; Kuhara, K.; Kudo, M.; Kodama, Y.; Dasgupta, P. K.; Toda, K. Electrodialytic ion isolation for matrix removal. *Anal. Chem.* **2012**, *84*, 5421−5426.

(24) Ohira, S.-I.; Sakaki, T.; Miyachi, R.; Otsubo, A.; Umemoto, A.; Kuwahara, Y.; Toda, K. Miniaturized crossflow ion transfer device for post-column enrichment in ion chromatography. *Talanta* **2020**, *216*, No. 120989.

(25) Nugraha, W. C.; Nagai, H.; Ohira, S.; Toda, K. Semi-continuous monitoring of Cr(VI) and Cr(III) during a soil extraction process by means of an ion transfer device and graphite furnace atomic absorption spectroscopy. *Anal. Sci.* **2020**, *36*, 617−620.

(26) Mori, M.; Sagara, K.; Arai, K.; Nakatani, N.; Ohira, S.; Toda, K.; Itabashi, H.; Kozaki, D.; Sugo, Y.; Watanabe, S.; Ishioka, N. S.; Tanaka, K. Simultaneous analysis of silicon and boron dissolved in water by combination of electrodialytic salt removal and ion-exclusion chromatography with corona charged aerosol detection. *J. Chromatogr. A* **2016**, *1431*, 131−137.

(27) Bjerrum, J. On the tendency of the metal ions toward complex formation. *Chem. Rev.* **1950**, *46*, 381−401.

(28) Bard, A. J.; Parsons, R.; Jordan, J. *Standard Potentials in Aqueous Solution*, 1st ed.; Marcel Dekker:New York, 1985; Vol. *287−293*, pp 321−328.

(29) Watanabe, S.; Iida, Y.; Suzui, N.; Katabuchi, T.; Ishii, S.; Kawachi, N.; Hanaoka, H.; Watanabe, S.; Matsuhashi, S.; Endo, K.; Ishioka, N. S. Production of No-Carrier-Added ^{64}Cu and Applications to Molecular Imaging by PET and PETIS as a Biomedical Tracer. *J. Radioanal. Nucl. Chem.* **2009**, *280*, 199−205.

(30) Watanabe, S.; Watanabe, S.; Liang, J.; Hanaoka, H.; Endo, K.; Ishioka, N. S. Chelating ion-exchange methods for the preparation of no-carrier-added [64]Cu. *Nucl. Med. Biol.* **2009**, *36*, 587−590.

(31) Ohya, T.; Nagatsu, K.; Suzuki, H.; Fukada, M.; Minegishi, K.; Hanyu, M.; Fukumura, T.; Zhang, M.-R. Efficient preparation of high-quality ^{64}Cu for routine use. *Nucl. Med. Biol.* **2016**, *43*, 685−691.